



EVROPSKÁ UNIE  
Evropské strukturální a investiční fondy  
Operační program Výzkum, vývoj a vzdělávání



## Výukový materiál

# F7DIBMC - Biophysical Modeling in Cardiology



ESC  
European Society  
of Cardiology

European Heart Journal - Digital Health (2022) 3, 169–180  
<https://doi.org/10.1093/ehjdh/ztac007>

ORIGINAL ARTICLE

## CineECG provides a novel anatomical view on the normal atrial P-wave

Emanuela T. Locati <sup>1</sup>, Carlo Pappone <sup>1,2</sup>, Francesca Heilbron <sup>3</sup>, and Peter M. van Dam <sup>4\*</sup>

<sup>1</sup>Department of Arrhythmology and Electrophysiology, IRCCS Policlinico San Donato, Milano, Italy; <sup>2</sup>University San Raffaele Vita & Salute, Milano, Italy; <sup>3</sup>IRCCS Istituto Auxologico, University of Milan, Milan, Italy; and <sup>4</sup>Department of Cardiology, University Medical Center Utrecht, Heidelberglaan 100, Utrecht, The Netherlands

Received 30 November 2021; revised 9 January 2022; accepted 3 February 2022; online publish-ahead-of-print 11 February 2022

### Aims

Novel *CineECG* computed from standard 12-lead electrocardiogram (ECG) correlated the ventricular electric activity to ventricular anatomy. *CineECG* was never applied to reconstruct the spatial distribution of normal atrial electric activity into an atrial anatomic model.

### Methods and results

From 6409 normal ECGs from PTB-XL database, we computed a median beat with fiducial points for P- and Q-onset. To determine the temporo-spatial location of atrial activity during PQ-interval, *CineECG* was computed on a normal 58-year-old male atrial/torso model. *CineECG* was projected to three major cardiac axes: posterior-anterior, right-left, base-roof, and to the standard cardiac four-chamber, left anterior oblique, and right anterior oblique (RAO) views. In 6409 normal subjects, during P-wave, *CineECG* moved homogeneously from right atrial roof towards left atrial base ( $-54 \pm 14^\circ$  in four-chamber view,  $95 \pm 24^\circ$  RAO view). During terminal PQ-interval, the *CineECG* direction was opposite, moving towards left atrial roof ( $62 \pm 27^\circ$  in four-chamber view,  $78 \pm 27^\circ$  RAO view). We identified the deflection point, where the atrial *CineECG* changes in direction. The time from P-onset to deflection point was similar to P-wave duration.

### Conclusion

*CineECG* provided a novel three-dimensional visualization of atrial electrical activity during the PQ-interval, relating atrial electrical activity to the atrial anatomy. *CineECG* location during P-wave and terminal PQ-interval were homogeneous within normal controls. *CineECG* and its deflection point may enable the early detection of atrial conduction disorders predisposing to atrial arrhythmias.

\* Corresponding author. Tel/Fax: +31 622198396, Email: [peter.van.dam@peics.nl](mailto:peter.van.dam@peics.nl)

© The Author(s) 2022. Published by Oxford University Press on behalf of the European Society of Cardiology.

This is an Open Access article distributed under the terms of the Creative Commons Attribution-NonCommercial License (<https://creativecommons.org/licenses/by-nc/4.0/>), which permits non-commercial re-use, distribution, and reproduction in any medium, provided the original work is properly cited. For commercial re-use, please contact [journals.permissions@oup.com](mailto:journals.permissions@oup.com)



## Výukový materiál

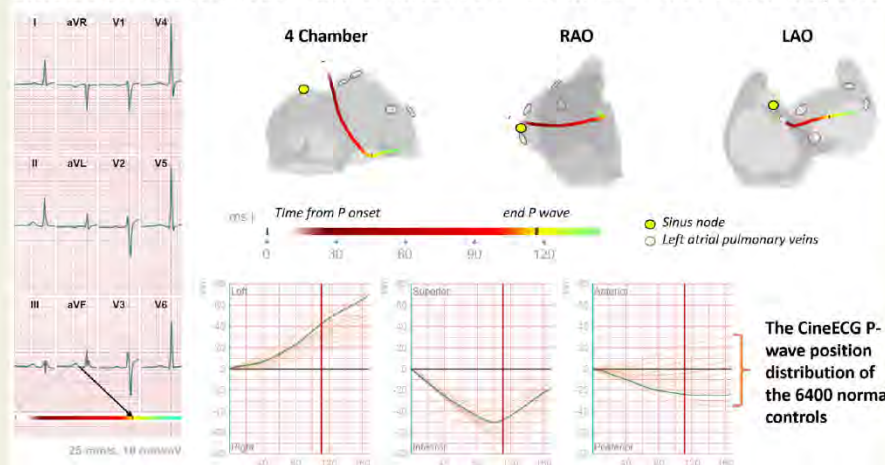
# F7DIBMC - Biophysical Modeling in Cardiology

170

E.T. Locati et al.

### Graphical Abstract

#### CineECG: Anatomical View on the Normal Atrial P Wave and beyond



### Keywords

Electrocardiogram • CineECG • Cardiac modelling • P-wave • Atrial depolarization • Terminal PQ activity

## Introduction

The normal atrial depolarization starts in the sinus node, often located close to the vena cava superior, and proceeds sequentially from right to left, with the right atrial roof activated before the left atrium.<sup>1,2</sup> The P-wave of the electrocardiogram (ECG) represents the electrical activation of the atria, where the right and left atrial activation waveforms summate to form the P-wave. The amplitude of the normal P-wave on the standard surface 12-lead ECG is generally rather small (maximum 0.2 mV), making it difficult to quantify the P-wave morphology.<sup>3,4</sup> It is even more difficult to visualize the atrial repolarization, which is generally associated with the interval between the P-wave onset to Q-wave onset.<sup>5,6</sup> Like in the ventricles, the local electrical gradients during atrial repolarization are much less steep than the depolarization gradients, as the repolarization is much slower than depolarization. At a difference with the ventricles, the atrial action potentials have a shorter plateau phase, due to a smaller calcium influx, then atrial repolarization starts earlier, and proceeds more gradually than ventricular repolarization.<sup>7</sup> Consequently, the depolarization forces prevail in the P-wave, and the repolarization is often not perceivable on the surface ECG with amplitudes  $<0.2$  mV,<sup>8</sup> at a difference with the ventricles where depolarization and repolarization are both evident, respectively represented by QRS and T waves.

In patients with atrial arrhythmias and atrial fibrillation, the P-wave during sinus rhythm can show subtle abnormalities, difficult to quantify by standard 12-lead ECG. Alterations of P-wave morphology may correlate with atrial remodelling and/or with the presence of atrial conduction delays, possibly due to fibrosis, and may be predictive of atrial arrhythmias and atrial fibrillation. As an example, broad, notched P-waves in lead 2, with deep and broad negative P terminal components in lead V1, are classically considered marker of left atrial enlargement, although other pathologic conditions, such as left atrial volume or pressure overload, interatrial conduction defect, or a combination of these abnormalities may also contribute to such abnormalities. Increased P-wave dispersion (PWD), defined as the difference between the longest and the shorter P-wave duration from the 12 ECG leads, is another non-invasive ECG marker for atrial anatomical remodelling.<sup>9</sup> Both increased P-wave duration and PWD reflect prolongation of intra-atrial and inter-atrial conduction. Patients with enlarged P-wave and with increased PWD may have a higher risk of developing atrial arrhythmias and atrial fibrillation, supporting that those ECG changes may reflect electrical and/or mechanical atrial remodelling.<sup>9,10</sup>

The novel CineECG, derived from the standard 12-lead ECG by an inverse ECG method, can correlate the atrial waveforms to the cardiac anatomy, obtaining a temporo-spatial correlation of the electrical activity with the anatomical location of the electrical source.



## Výukový materiál

# F7DIBMC - Biophysical Modeling in Cardiology

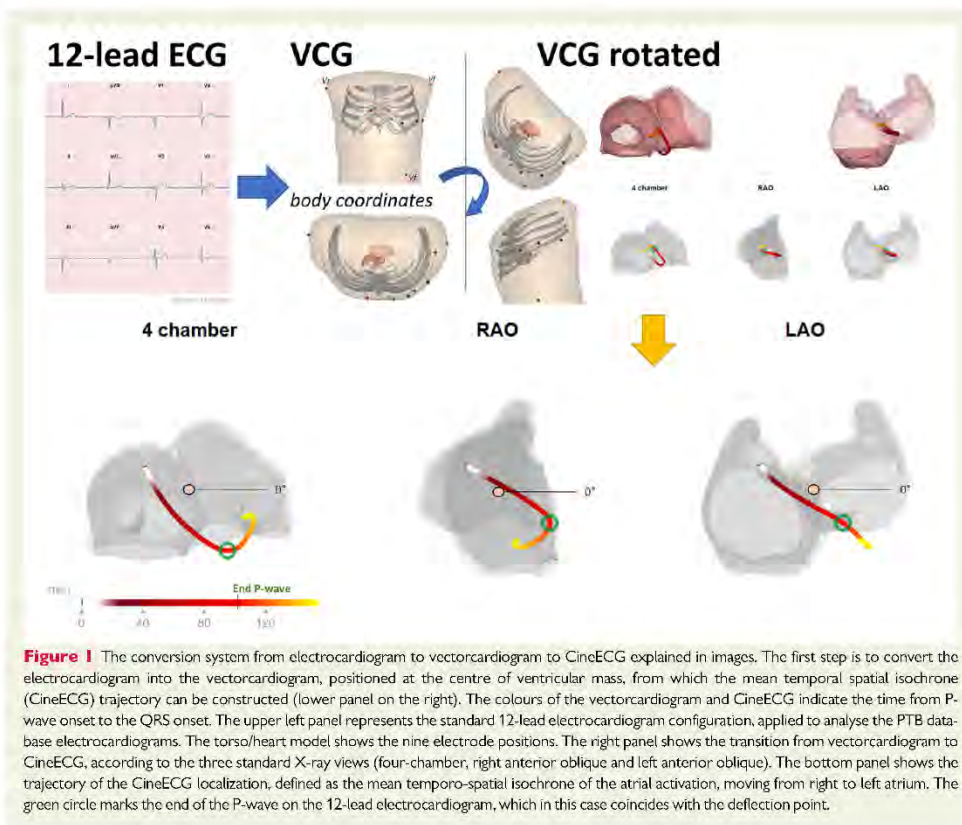


**Figure 1** The conversion system from electrocardiogram to vectorcardiogram to CineECG explained in images. The first step is to convert the electrocardiogram into the vectorcardiogram, positioned at the centre of ventricular mass, from which the mean temporal spatial isochrone (CineECG) trajectory can be constructed (lower panel on the right). The colours of the vectorcardiogram and CineECG indicate the time from P-wave onset to the QRS onset. The upper left panel represents the standard 12-lead electrocardiogram configuration, applied to analyse the PTB database electrocardiograms. The torso/heart model shows the nine electrode positions. The right panel shows the transition from vectorcardiogram to CineECG, according to the three standard X-ray views (four-chamber, right anterior oblique and left anterior oblique). The bottom panel shows the trajectory of the CineECG localization, defined as the mean temporo-spatial isochrone of the atrial activation, moving from right to left atrium. The green circle marks the end of the P-wave on the 12-lead electrocardiogram, which in this case coincides with the deflection point.

We already demonstrated the feasibility and clinical relevance of CineECG in the study of patients with intraventricular conduction blocks (left bundle branch block and right bundle branch block) and in patients with Brugada syndrome,<sup>11</sup> however the CineECG method was never applied yet to the atrial activity.

The objective of this study was to explore and quantify the normal atrial activation by the novel CineECG methodology, with the aim to correlate the ECG signals occurring during the P-wave and PQ-interval to the atrial anatomy.

## Methods

### CineECG method

The CineECG method quantifies the mean temporo-spatial localization of the normal cardiac electrical activity, including both depolarization and repolarization.<sup>12</sup> The CineECG method has been already described in detail elsewhere.<sup>11,13-15</sup> In summary, the CineECG relates the cardiac activation and recovery pathway to the cardiac anatomy, using the torso/heart

model of a 57-year male, with average body build relative to the study population (see Figure 1). However, in those previous studies, the model only included the ventricles, while for this study the torso/heart model also included the atria. The torso/heart model was used to derive the vectorcardiogram (VCG) from the recorded 12-lead ECG, assuming the electrode positions using the method described by van Dam.<sup>15</sup> The VCG was subsequently used to compute the CineECG, estimating the mean temporo-spatial isochrone.<sup>15</sup>

The VCG direction was utilized to compute the CineECG trajectory, depicting the localization of the average electrical activity of the atria at each given time interval. The VCG direction is the unit vector of the normalized VCG signal ( $\frac{VCG(t)}{VCG(t)}$ ). Normal atrial activation starts in the sinus node, located close to the superior vena cava, moving from there through the atrial tissue (Figure 1). To localize the CineECG trajectory within the atrial anatomy, the mid P-wave location was set to the centre of the mass of the atrial model. This site represents the centre of electrical atrial activation, when approximately half of the atrial mass is activated. From this site, the subsequent CineECG cardiac locations are computed during the entire P-wave and PQ-interval according to the following equations:



## Výukový materiál

# F7DIBMC - Biophysical Modeling in Cardiology

**Table 1** Demographics and results of the normal atrial CineECG in six-decade age groups by sex<sup>a</sup>

AGE (years)	Sex	N	P-wave duration (ms)	Deflection point (ms)	PQ interval (ms)	P-wave four-chambers (grades)	P-wave RAO (grades)	P-wave LAO (grades)	Terminal PQ four-chambers (grades)	Terminal PQ RAO (grades)	Terminal PQ LAO (grades)
18–29	Females	456	103 ± 10	119 ± 21	145 ± 19	-60 ± 10	94 ± 20	6 ± 28	65 ± 30	-86 ± 49	8 ± 64
	Males	275	109 ± 12	109 ± 25	153 ± 19	-59 ± 16	93 ± 27	7 ± 30	60 ± 23	-82 ± 34	-11 ± 45
30–39	Females	382	104 ± 10	115 ± 25	149 ± 20	-59 ± 11	95 ± 19	9 ± 30	66 ± 26	-86 ± 35	-1 ± 58
	Males	382	112 ± 12	109 ± 23	158 ± 20	-56 ± 13	93 ± 24	5 ± 26	58 ± 23	-83 ± 34	-7 ± 38
40–49	Females	627	107 ± 10	115 ± 24	151 ± 20	-57 ± 11	96 ± 24	9 ± 26	64 ± 30	-81 ± 41	-8 ± 55
	Males	522	114 ± 12	108 ± 24	160 ± 21	-54 ± 13	95 ± 21	5 ± 24	57 ± 26	-76 ± 41	-10 ± 38
50–59	Females	751	110 ± 12	113 ± 26	156 ± 20	-54 ± 12	95 ± 24	8 ± 25	65 ± 24	-81 ± 36	-13 ± 52
	Males	664	116 ± 13	107 ± 24	163 ± 21	-53 ± 14	94 ± 24	5 ± 25	57 ± 27	-76 ± 39	-13 ± 41
60–69	Females	630	113 ± 12	114 ± 28	160 ± 21	-54 ± 12	97 ± 21	9 ± 25	67 ± 26	-79 ± 34	-20 ± 55
	Males	559	119 ± 13	107 ± 26	169 ± 21	-51 ± 13	97 ± 24	8 ± 24	57 ± 28	-73 ± 39	-18 ± 43
70–100	Females	773	114 ± 15	107 ± 30	166 ± 23	-52 ± 16	96 ± 26	11 ± 27	65 ± 30	-72 ± 44	-23 ± 58
	Males	338	121 ± 16	107 ± 30	171 ± 32	-47 ± 23	93 ± 41	10 ± 29	58 ± 30	-70 ± 38	-23 ± 44
18–100	Females	3619	110 ± 13	113 ± 26	155 ± 22	-53 ± 15	95 ± 27	7 ± 26	65 ± 28	-80 ± 40	-12 ± 58
	Males	2790	116 ± 13	107 ± 25	163 ± 23	-57 ± 13	95 ± 27	9 ± 27	58 ± 27	-76 ± 38	-14 ± 42
Total		6409	112 ± 12	110 ± 26	159 ± 23	-54 ± 14	95 ± 24	8 ± 26	62 ± 27	-78 ± 27	-13 ± 51

<sup>a</sup>More detailed information on P-wave duration, deflection point, and PQ-interval, including significance values, between sex and age groups are provided in [Supplementary material online, Appendix A](#)

$$\text{CineECG}(t) = \text{CineECG}(t-1) - v \cdot dt \cdot \frac{\text{VCG}(t)}{|\text{VCG}(t)|} \quad t < \text{midPwave}$$

$$\text{CineECG}(t) = \text{center of atrial mass } t = \text{midPwave}$$

$$\text{CineECG}(t) = \text{CineECG}(t-1) + v \cdot dt \cdot \frac{\text{VCG}(t)}{|\text{VCG}(t)|} \quad t > \text{midPwave}$$

in which  $v$  is the speed by which the CineECG travels through the atrial anatomy, and  $dt$  is the time step, in this case 1 ms. The speed of 0.7 m/s is chosen as in the physiological range of the myocardial propagation velocity.<sup>16,17</sup>

To visualize and establish a quantifiable relation between the atrial anatomy and the VCG/CineECG trajectory, the VCG is rotated towards the three heart axes: ( $x$ ) from right to left, ( $y$ ) from the roof to the base, and ( $z$ ) from posterior to anterior. The CineECG was projected to three standard X-ray views of the heart: the standard four-chamber view, and the right anterior oblique and left anterior oblique (RAO and LAO) views (Figure 1). The direction and the position of the CineECG can now be related to atrial anatomy.

### The atrial CineECG waveform in relation to ECGsim atrial activation map

We compared the atrial activation waveforms obtained by CineECG with the atrial activation map provided by the open source simulation tool ECGsim ([www.ecgsim.org](http://www.ecgsim.org)).<sup>18</sup> The atrial activation sequence provided by ECGsim was estimated using an inverse ECG procedure using a body surface map (BSM) with 67 ECG signals.<sup>19</sup> The ECGsim atrial activation isochrones was used to interpret the CineECG pathway. Of note, the ECGsim showed the atrial activation of a normal young male (20 years), with slender body build with a vertical heart orientation. For this case, we

also computed his CineECG, using the measured 12-lead ECG as well as the provided atrial torso/heart model.

### Electrocardiogram study dataset

As source of normal atrial activation, we utilized the 6668 ECGs labelled as healthy controls included in the certified Physionet PTB Diagnostic ECG Database <https://www.physionet.org/content/ptbdb/1.0.0/>.<sup>20</sup> From those ECGs, we excluded 259 ECGs, for the following reasons:

- The ECG was excessively noisy, preventing the construction of a median beat or reliably detecting the P-wave fiducials (222 ECGs).
- the PQ-interval duration was shorter than 80 ms (32 ECGs), and
- the P-wave polarity was negative in Lead 2 (5 ECGs).

Therefore, our ECG study dataset included 6409 ECGs, used for the construction of the normal atrial CineECG. Each analysed ECG was assigned to an age and a gender group according to the information provided by the PTB XL database (Table 1).

### Twelve-lead electrocardiogram and CineECG parameters used to characterize atrial activity

From each 10-s 12-lead ECG, a median beat is automatically constructed by CalECG/bravo.<sup>21,22</sup> The P-wave fiducial points were automatically determined with the same software. To characterize the different characteristics of the P-wave on 12-lead ECG, and the different CineECG patterns, the following ECG and CineECG parameters are utilized:

#### PQ-interval parameters

We determine the duration of the PQ-interval, from the onset of the P-wave to the onset of the Q-wave, from the 12-lead automatically



## Výukový materiál

# F7DIBMC - Biophysical Modeling in Cardiology

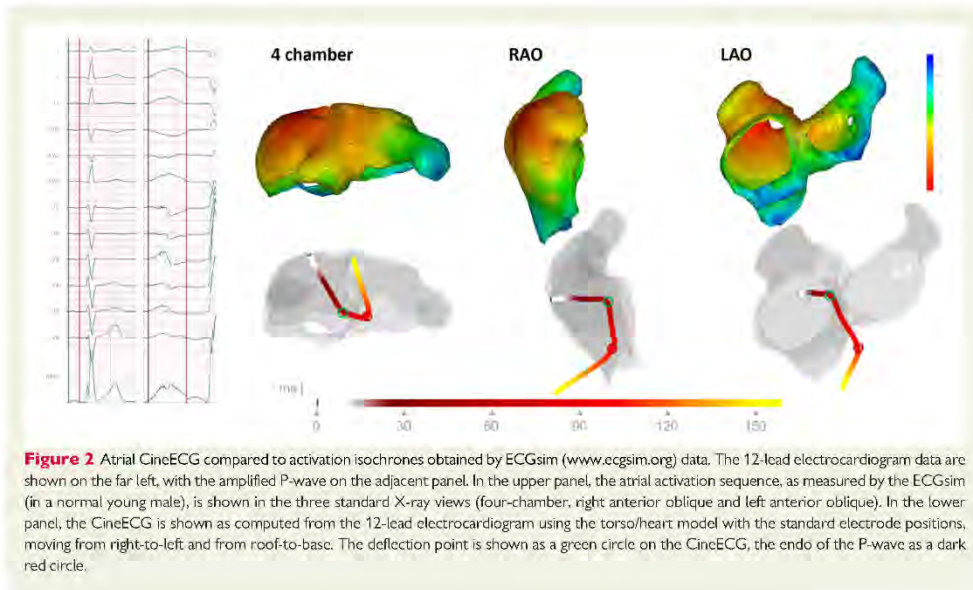


**Figure 2** Atrial CineECG compared to activation isochrones obtained by ECGsim ([www.ecgsim.org](http://www.ecgsim.org)) data. The 12-lead electrocardiogram data are shown on the far left, with the amplified P-wave on the adjacent panel. In the upper panel, the atrial activation sequence, as measured by the ECGsim (in a normal young male), is shown in the three standard X-ray views (four-chamber, right anterior oblique and left anterior oblique). In the lower panel, the CineECG is shown as computed from the 12-lead electrocardiogram using the torso/heart model with the standard electrode positions, moving from right-to-left and from roof-to-base. The deflection point is shown as a green circle on the CineECG, the end of the P-wave as a dark red circle.

detected fiducial points. We then divided the PQ-interval into the following two sections:

- *P-wave duration*: The P-wave duration, from P-wave onset to P-wave end.
- *Terminal PQ-interval*: from P-wave end to Q-wave onset.

### P-wave direction angle

The direction of the CineECG trajectory during the P-wave was computed according to the three standard cardiac views (Figure 1). The direction was defined as the position at the P-wave end minus the position at the P-wave onset. Based on this direction, the P-wave angle direction was computed relative to the positive x-axis, where  $0^\circ$  is defined as the positive x-axis per heart view (four-chamber, RAO, or LAO) (see Figure 1).

### P-wave deflection point

The P-wave deflection point is defined as the time when the CineECG direction deviates more than  $60^\circ$  from the average CineECG direction of the initial ( $n$ ) 30 ms of the atrial activation. From the ECGsim example of the CineECG, the first deflection point was found at 56 ms (see Figure 2).

$$\overrightarrow{\text{CineECG}_{\text{nsd}}} = \frac{1}{n} \sum_{t=1}^n \frac{\text{VCG}(t)}{|\text{VCG}(t)|}$$

$$\text{P-wave direction angle} = \arccos \left( \frac{\text{VCG}(t)}{|\text{VCG}(t)|} \cdot \overrightarrow{\text{CineECG}_{\text{nsd}}} \right)$$

Find  $t_{\text{deflection}}$  in P-Q interval for which P-wave direction angle is larger than  $60^\circ$ , consequently  $t_{\text{deflection}}$  is limited to the PQ-interval and larger than  $n$  ( $=30$  ms).

### Statistical analysis

Statistical analysis was performed by SPSS (IBM SPSS Statistics for Windows, Version 26.0.0.1, Armonk, NY, USA: IBM Corp.). Data were given as mean  $\pm$  standard deviation (SD), and ranges (minimum–maximum), for variables with normal distribution, and mean  $\pm$  SD, median and ranges for nonparametric variables. Kruskal–Wallis nonparametric test on independent samples was used to analyse differences between gender and age-groups by decades, significance values were adjusted by the Bonferroni correction for multiple tests. A 0.05 significance level was used, applying Bonferroni correction for repeated comparisons. The complete statistical analysis was provided in [Supplementary material online, Appendix A](#).

## Results

### The atrial CineECG in relation to the atrial map derived from the ECGsim model

The normal atrial activation map provided by the ECGsim of the 'normal young male' was shown in Figure 2, according to the three standard X-ray views, together with the atrial CineECG computed in the same subject. In the ECGsim map, the atrial isochrones show an initial breakthrough at the sinus node region, located in the upper right atrium, close to the superior vena cava. From there, the activation spreads in all directions. At 56 ms after breakthrough, the right atrial appendage was activated, resulting in isochrones progressing towards the inferior vena cava and to the left appendage. The atrial CineECG mirrors the atrial activation pattern shown by the ECGsim, as initially



## Výukový materiál

# F7DIBMC - Biophysical Modeling in Cardiology

the *CineECG* moves from the roof towards the base of the atria for the first 50–60 ms, then the *CineECG* bends towards the left base region. We defined this bending as the 'deflection point', occurring around 50–60 ms after the P-wave onset. Noteworthy, *CineECG* still measured electrical activity beyond 120 ms, beyond the P-wave end, during the terminal PQ-interval, a time interval not included in the *ECGsim* model. During the terminal PQ-interval, which on the surface 12-lead ECG reaches a maximum of much less than 0.05 mV, the *CineECG* shows a consistent direction moving at a sharp angle compared to the P-wave direction, mainly from the atrial base to the atrial roof and from left to right atrium. It is possible that such direction may represent the atrial repolarization, or in alternative, a late depolarization of the left atrium.

### Atrial *CineECG* activity during P-wave and PQ-interval in the PTB database electrocardiogram tracings

The average *CineECG* locations during the P-wave and the PQ-interval, obtained in 6409 ECG tracings from PTB database included in the study set, were plotted along each three cardiac axes (Figure 3). The *CineECG* tempo-spatial location and direction were quite homogeneous in those normal ECG tracings, particularly during the P-wave, when also the differences between age and gender groups were limited (Figure 3, Table 1). The complete results of the statistical analysis by sex and age classes are provided in [Supplementary material online, Appendix A](#). The P-wave duration tended to be longer with increasing age, in both sexes, and particularly within males, often lasting more than 120 ms above age 70 years (Table 1). Also, the PQ-interval was about 20 ms longer in subjects above age 70 years in both sexes, when compared with younger subjects.

### Time and location of the deflection point

In ~90% of the normal subjects, in both sexes, we observed that the *CineECG* makes a sharp turn, that we defined as the 'deflection point', located close to the base near the interatrial septum. In ~80% of the subjects, the deflection point occurs within 25 ms before or after the P-wave end, occurring earlier with increasing age, particularly in females (Table 1, [Supplementary material online, Appendix A](#)).

The distribution of the *CineECG* temporo-spatial locations during entire PQ-interval derived from the 6409 normal atrial ECG tracings was used to create the normal distribution of the atrial electric activity (Figure 4). The *CineECG* location relative to the three cardiac axes during the PQ-interval was plotted as orange lines representing the 90% range (with 5–95% confidence intervals), as derived from the 6409 normal ECG tracings. The normal range for *CineECG* locations was then used to compare the behaviour of a single *CineECG* tracing in relation to the normal range. Figure 4, top panel, shows the behaviour of an individual with normal atrial *CineECG*, with P-wave duration of 95 ms, and deflection-point occurring at 105 ms, all parameters being well within normal ranges (Table 1).

### P-wave direction angles

The P-wave direction angles per heart view, either four-chambers, RAO, and LAO projections are shown as histograms in Figure 5 (upper panels). The spatial distribution in relation to the atrial anatomy within the 5–95% angle range is shown in Figure 5 (bottom

panels). In these normal subjects, the P-wave direction had very limited variation, moving the roof of the atrium (the sinus node area) towards the left atrial base (Figure 5 (upper panels)). The average direction was  $56 \pm 12^\circ$  in the four-chamber view,  $98 \pm 22^\circ$  in the RAO view, and  $10 \pm 27^\circ$  in the LAO view (Table 1). The atrial *CineECG* average direction was very similar for males and females (Table 1, [Supplementary material online, Appendix A](#)).

### Atrial *CineECG* in subjects from PTB database with deviations from the normal distribution

Within the 6409 ECG tracings included in the study dataset, we identified only six subjects (all males aged over 60 years), with an apparently normal P-wave on 12-lead ECG, in whom the *CineECG* deviated from the normal *CineECG* atrial distribution. In these subjects, the deflection point occurred well before the P-wave end, pointing sharply to the left atrium at less than 50 ms after the P-wave onset. Thus, in these subjects, most of the electrical atrial activity appear to be located in the left atrium. An example of a subject (PTB-XL ECG-ID: 754<sup>23</sup>) in whom the atrial activity moved earlier and stayed longer in the left atrium, despite an apparently normal P-wave on the 12-lead ECG, is shown in Figure 4 (middle panel).

Besides, we also observed five ECGs tracings with inverted P-wave in Lead 2, which we excluded from the study dataset used to define the normal *CineECG* distribution. Among them, the atrial activation started near the base of the septum rather than in the right atrial roof, and it ended in the right atrium, rather than in the left atrium. The ECG of one of those subjects (PTB-XL ECG-ID: 6488<sup>23</sup>) is shown in Figure 4 (bottom panel).

Within the PTB-XL database, we also detected a few ECG tracings with at least one premature atrial contraction (PAC). In those tracings, we observed that the sinus P-wave showed a normal *CineECG* trajectory, while the ectopic P-wave showed an abnormal *CineECG* trajectory. We show an example illustrating the differences between the sinus P-wave and the ectopic P-wave (Figure 6, ECG-ID: 18115 of the PTB-XL database<sup>23</sup>). The sinus P-wave *CineECG* shows a normal trajectory, starting near the right atrial roof and travelling towards the left base and moving leftward only in the terminal PQ-interval. The ectopic P-wave *CineECG*, however, starts from the left atrial roof, and then moves almost in a straight line towards the right base. Interestingly, in this case, the *CineECG* followed the same abnormal trajectory both during the ectopic P-wave and during the terminal PQ-interval, without an evident deflection point.

## Discussion

This study showed that the *CineECG* is a valuable tool in describing the tempo-spatial localization of the atrial activity, as well as it did for the ventricular activity.<sup>12</sup> In the normal ECG tracings included in the PTB XL database, the *CineECG* univocally showed that the normal atrial activation starts in the right upper atrium, and subsequent spreads simultaneously from the roof to the base of the right and left atria.

We found limited variations in the atrial activity pathway during the PQ-interval among the gender/age groups (Figure 3, Table 1). The



## Výukový materiál

### F7DIBMC - Biophysical Modeling in Cardiology

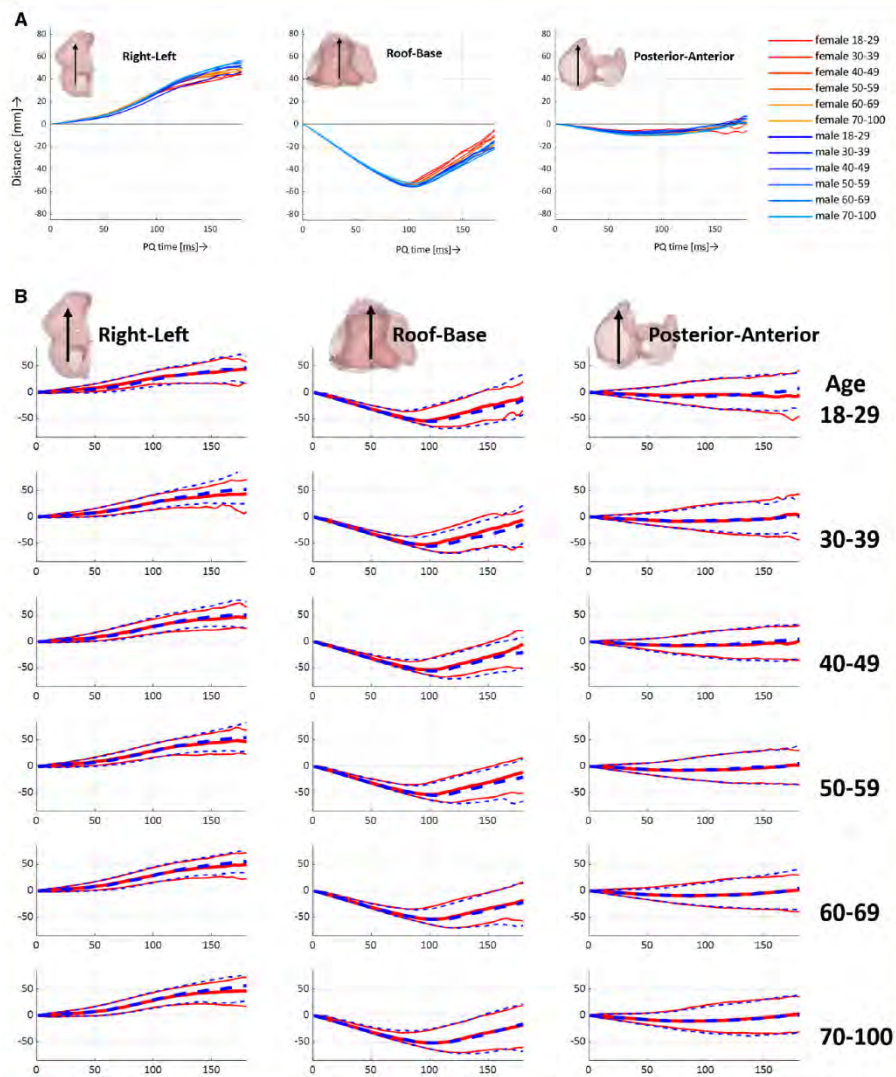


**Figure 3** Normal atrial CineECG temporo-spatial locations for age and gender groups by the three cardiac axes. On the upper panel (A), the mean CineECG trajectories superimposed for gender and age classes by decades, according to the three cardiac axes (right-left view on the right, roof-to-base view in the middle, and posterior-anterior view on the left). The deflection point is especially visible in the roof-to-base view. In the lower panels (B), the mean CineECG trajectories (continuous red lines for females, blue dashed lines for males) with 5–95% range by age classes by decades.



## Výukový materiál

# F7DIBMC - Biophysical Modeling in Cardiology

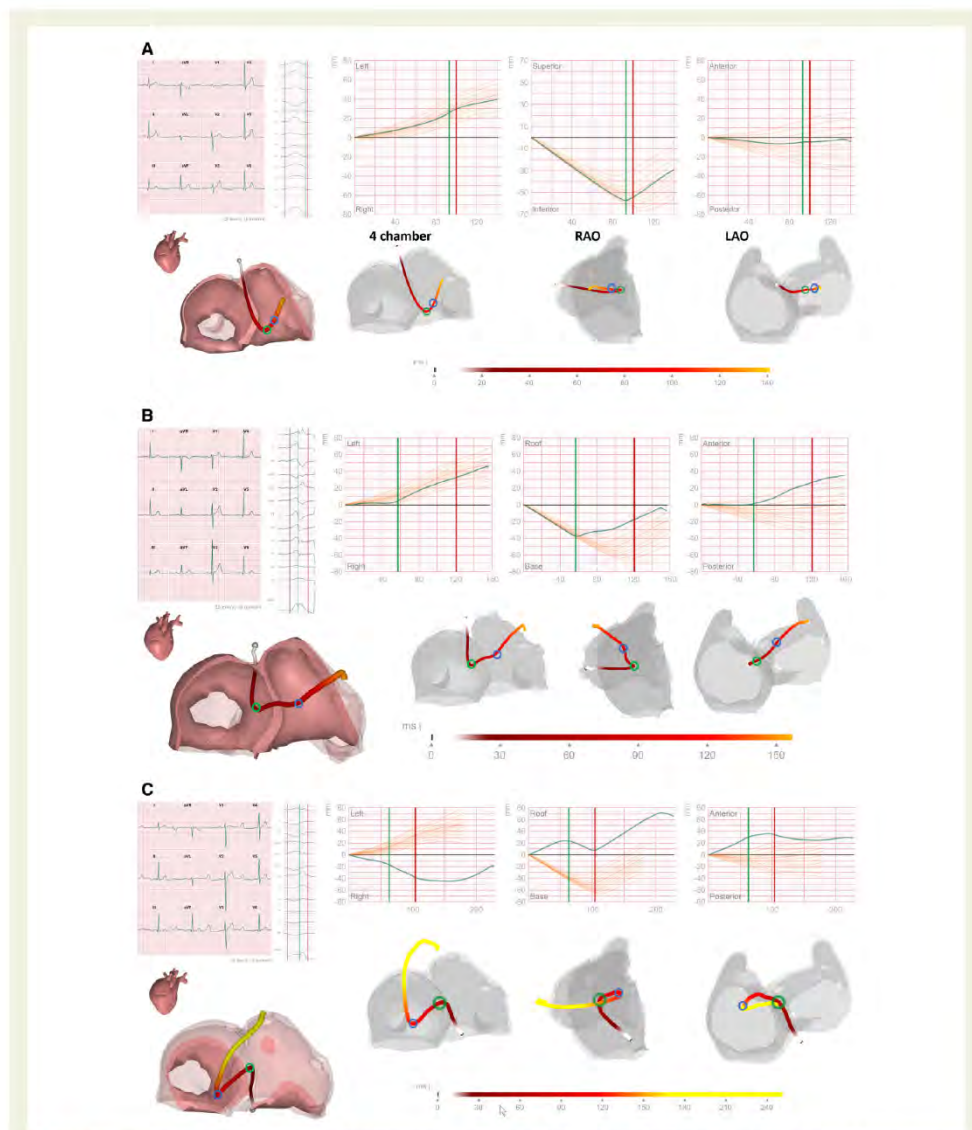


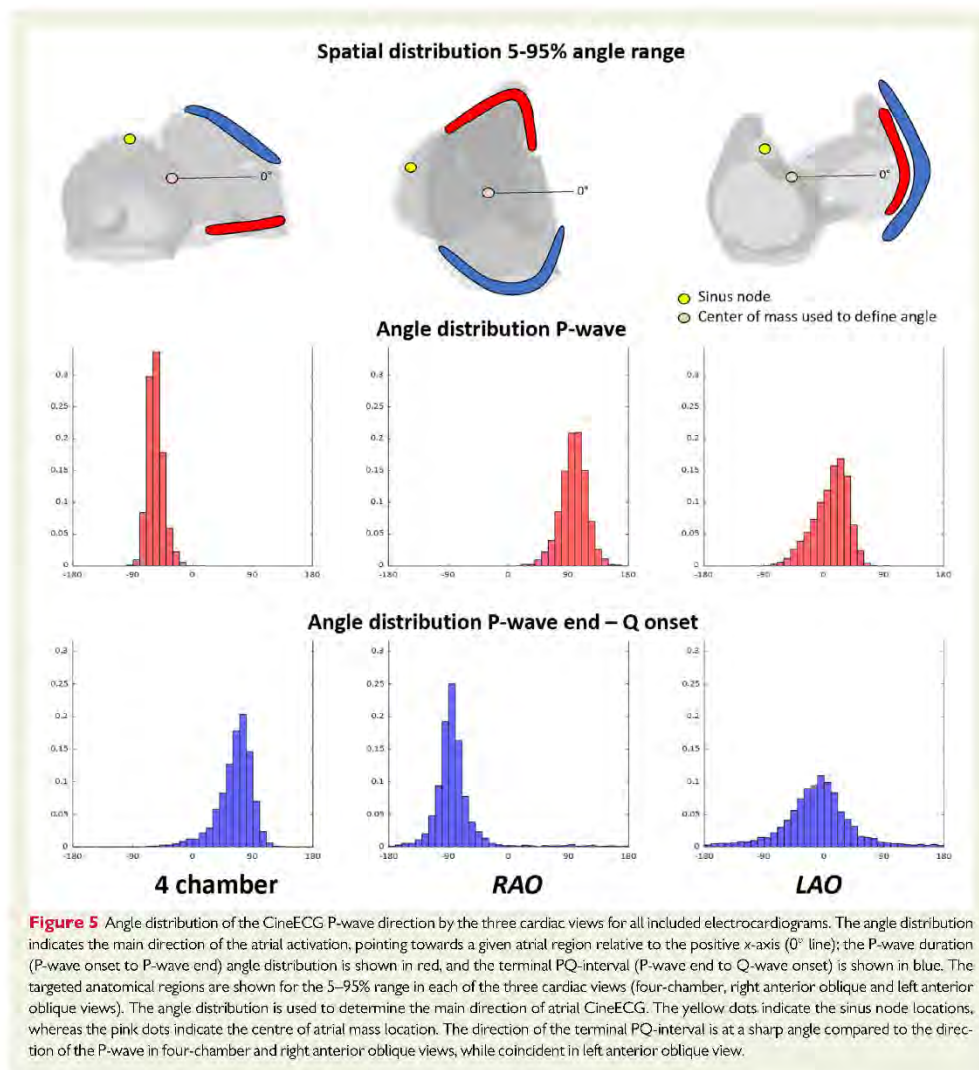
**Figure 4** Normal distribution of the CineECG atrial trajectories derived from the 6409 electrocardiogram analysed tracings, according to the three cardiac axes. In upper panel A, the distribution of the CineECG temporo-spatial locations during PQ-interval derived from all 6409 normal atrial electrocardiogram tracings were used to create a normal distribution of the CineECG during the entire atrial activity. The normal PQ-interval position distribution was plotted as orange lines representing the 90% range (with 5–95% confidence intervals) of the normal. In panel C, the behaviour of a single normal CineECG atrial trajectory, moving from right-to-left, and from roof-to-base. The time scale moves from dark red to yellow. The green circles indicate the deflection point, and the blue circle the end of the P-wave. In the mid panel B, the CineECG atrial trajectory of a subject with apparently normal P-wave duration, but with short duration at deflection point (43 ms), in whom the initial atrial activation was mainly located in the right atrium towards the base, that later moved towards the left atrium. In the lower panel, the CineECG atrial trajectory of a subject excluded from the 6409 tracings used to construct the normal distribution of the CineECG atrial trajectories, as having a negative P-wave on the surface electrocardiogram. In this case, the atrial activation was mainly located in the right atrium, and the main direction of atrial activation moves from left to right, from base to roof, and from posterior to anterior.





## Výukový materiál

# F7DIBMC - Biophysical Modeling in Cardiology



P-wave duration and PQ-interval tended to be longer with increasing age, in both sexes, and particularly in males, when compared with younger subjects (Supplementary material online, Appendix A). Also, the deflection point, indicating the change in CineECG direction, had a homogeneous temporo-spatial location, as it was located close to the atrial base, near the interatrial septum, and generally occurred within 25 ms before or after the P-wave end, without significant differences by age and sex (Table 1).

### Trajectories of the normal atrial CineECG

The CineECG, using a standard atrial/torso model, showed that the average normal atrial activity started close to the roof of the right atrium and moved towards the left atrial base. The atrial activation pathway described by CineECG was consistent with the atrial activation isochrone map provided by the ECGsim simulator, showing a single focal atrial activation in the right upper atrium, subsequently spreading first to the right atrium, and later to left atrium. The exact



## Výukový materiál

### F7DIBMC - Biophysical Modeling in Cardiology

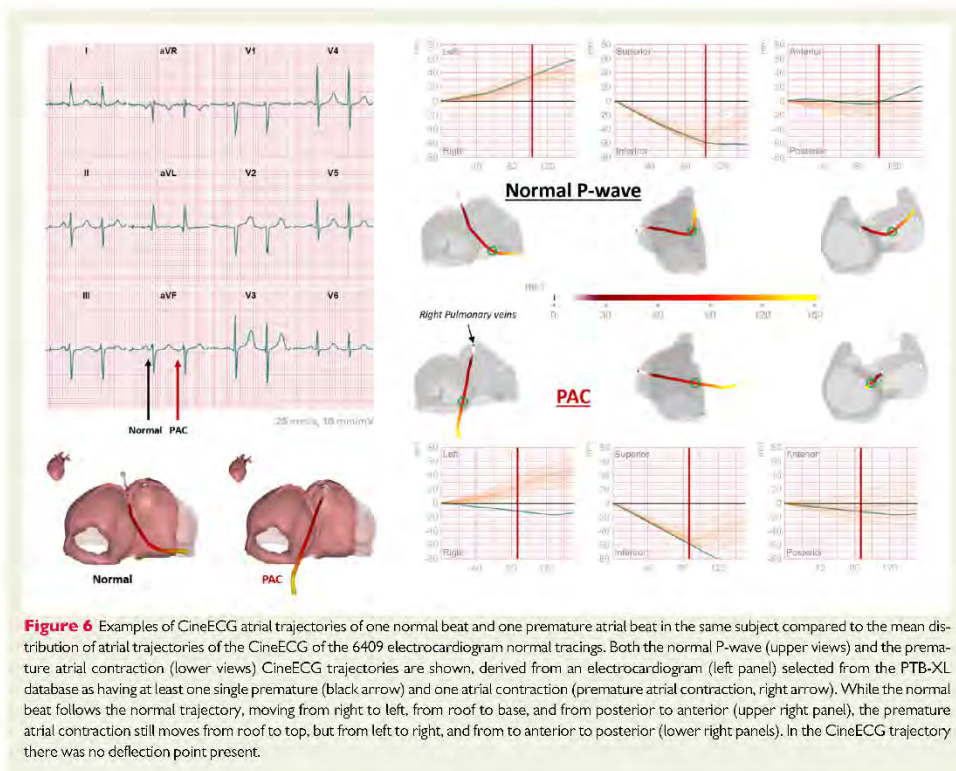


**Figure 6** Examples of CineECG atrial trajectories of one normal beat and one premature atrial beat in the same subject compared to the mean distribution of atrial trajectories of the CineECG of the 6409 electrocardiogram normal tracings. Both the normal P-wave (upper views) and the premature atrial contraction (lower views) CineECG trajectories are shown, derived from an electrocardiogram (left panel) selected from the PTB-XL database as having at least one single premature (black arrow) and one atrial contraction (premature atrial contraction, right arrow). While the normal beat follows the normal trajectory, moving from right to left, from roof to base, and from posterior to anterior (upper right panel), the premature atrial contraction still moves from roof to top, but from left to right, and from anterior to posterior (lower right panels). In the CineECG trajectory there was no deflection point present.

location of the atrial breakthrough varied slightly among the individual subjects; however this aspect needs further specific study, controlling the ECG electrode positions, and the body build and a atrial anatomy for the individual patient.

The CineECG detected consistent atrial activity beyond the end of the P-wave, during the PQ-interval, a segment which is almost isoelectric, thus uninformative, in the standard 12-lead ECG tracings. The CineECG often showed a deflection point close to the end of the P-wave after which the CineECG moved from the base towards the left roof of the atria during the terminal PQ-interval, thus in an opposite direction when compared with the CineECG during the P-wave moving from the roof to the base of the atria (Figure 5).

#### The significance of the CineECG deflection point

We showed that in 80% of the normal subjects, the atrial CineECG showed a clear deflection point close to the end of the P-wave, where the direction of the CineECG trajectory changed by an angle of more than  $60^\circ$  compared to its average initial direction. The presence

of a deflection point in the CineECG trajectory may have two possible alternative origins:

- an anatomical origin, due to anatomical or functional obstacles associated to intra-atrial structures and connections, and
- an electrical origin, indicating the transition from atrial depolarization to repolarization.

An example of a possible anatomical origin of the deflection point is suggested by the ECGsim example (Figure 2), where the deflection point is found after 56 ms, since there is no further atrial tissue to be activated in the roof to base direction. Consequently, the activation direction has to change its direction, as reflected by the CineECG. Another example of a possible anatomical origin is shown in Figure 4 (middle panel), where an intra-atrial conduction disorder might cause an early occurring deflection point. In this case, we made the hypothesis that the intra-atrial right-left connections at the roof level are non-functional, causing a sharp bend of the CineECG at the moment the activation reaches a functional right-left connection.<sup>24,25</sup>

Earlier experimental studies using monophasic action potentials, showed that the atrial repolarization follows the depolarization



## Výukový materiál

# F7DIBMC - Biophysical Modeling in Cardiology

trajectory,<sup>26</sup> consequently in all likelihood the atrial T-wave should be discordant, i.e. should have opposite polarity, than the P-wave. At a difference to what occurs during normal ventricular activity, where QRS and T waves have generally concordant polarity, the atrial activity acts similarly to what occurs during ventricular ectopic beats or in left bundle branch block, where T waves have generally opposite polarity compared to the QRS. In CineECG, similar to VCG, when the repolarization forces get dominant, a change of direction occurs. Thus, this supports the hypothesis of a possible electrical origin of the deflection point, at least in most normal subjects, where the deflection point occurs close to the end of the P-wave, thus most likely representing the transition from depolarization to repolarization. The activity occurring after the deflection point, during the terminal PQ-interval, might thus represent the atrial repolarization, as also described in other studies.<sup>4,8,27,28</sup>

So far, atrial repolarization has been seldom considered clinically, never described by an inverse ECG technique, and mostly in research studies with small populations.<sup>4,5,8,27,28</sup> This original finding by the novel CineECG method, may open new perspectives for the anatomical or electrical interpretation of abnormalities of atrial activity, regarding not only depolarization, but also repolarization.

Further studies, comparing invasive atrial mapping data with the CineECG, are needed to understand the origin of the deflection point, or to explain the absence of a deflection point, which we observed in a few cases still ostensibly normal, which might though indicate some hidden abnormalities (Figure 5).

### Abnormality of the CineECG deflection point

In case of an early deflection point, as shown in Figure 6 (middle panel), the CineECG moved initially from the right atrial roof towards the right base, then after 40ms it suddenly bended to the left. We hypothesized that this abrupt change of CineECG trajectory may depend on a possible disconnection between the right and left atrium, as it may occur in case of an intra-atrial conduction block, due to a dysfunctional connection between the right and left atrium at the roof level.<sup>29</sup> Clearly, this issue must be explored by studies also considering atrial dimensions measured by echocardiography and comparing the CineECG trajectory with simultaneous intracavitary atrial activation mapping.

### CineECG findings in premature atrial contractions (PAC)

We preliminarily explored the CineECG trajectory of a premature atrial contraction (PAC) compared to a normal sinus activation in the same ECG tracing. Interestingly, we observed that while the sinus P-wave followed the normal distribution, the ectopic P-wave showed a different trajectory, going from posterior left atrium to anterior right atrium (Figure 6). We also observed different pathways followed by the ectopic P-wave in the few cases we have explored yet, in all cases the ectopic P-wave CineECG did not show an deflection point as uniformly observed in normal beats. These preliminary observations need to be further explored in larger dedicated studies.

### Limitations

The focus of this article was to show the normal atrial electrical activity, and almost unexpectedly this led us to discover that not only depolarization forces but also forces likely to be attributed to the atrial repolarization could be estimated by the CineECG method, simply derived from the surface ECG. Of course, these observations will require a validation by atrial invasive mapping, which will be part of a future project. Such validation study is also required to determine the ability of CineECG to distinguish between different types of interatrial breakthrough and P-wave morphology, as shown by Holmqvist *et al.*<sup>30</sup> The validation study will also allow a better understanding of what we now define as the 'deflection point'.

Another study limitation is the use of a standardized torso/heart model, and additional studies need to confirm these results, preferably with a method using personalized torso/heart model. Another limitation of this study is the lack of echocardiographic data providing atrial dimensions, not available in the PTB-XL database. In the future, the accuracy of the CineECG locations in the atria might be improved by using a personalized atrial/torso model, maybe based on three-dimensional (3D) imaging based upon a 3D camera and/or 3D echocardiography. The correlation between CineECG and atrial anatomy, studied by two-dimensional and 3D echocardiography, need to be explored in dedicated future studies, especially to establish the relationship between atrial enlargement and changes in CineECG position and direction in patients with atrial conduction disorders and with atrial arrhythmias.

### Conclusions

The atrial CineECG showed that the atrial activity during the P-wave uniformly moves from the roof of the right atrium towards the left base in the vast majority of the 6409 normal ECGs included from the PTB-XL database. Furthermore, CineECG detected the presence of consistent atrial electrical activity beyond the end of the P-wave, during the terminal PQ-interval. The significant change in direction of the CineECG, defined as the deflection point, generally occurred close to the end of the normal P-wave and was located at the left atrial base. The deflection point may be due to either an anatomical or functional obstacle, or it may indicate the transition between atrial depolarization and repolarization. Abnormalities in the deflection point, both in time and location, were rare among the normal subjects. Vice versa, abnormalities in the CineECG deflection point in time and localization might be a marker of intra-atrial conduction disturbances and of susceptibility to atrial arrhythmias.

### Supplementary material

Supplementary material is available at *European Heart Journal – Digital Health* online.

### Funding

This work was supported by the Dutch Heart Foundation (QRS-Vision 2018B007).



## Výukový materiál

# F7DIBMC - Biophysical Modeling in Cardiology

180

E.T. Locati et al.

**Conflict of interest:** P.M. van Dam is an owner of ECG Excellence BV and Peacs BV.

### Data availability

The data underlying this article are available in: <https://physionet.org/content/ptb-xl/1.0.0/>.

### References

1. De Ponti R, Ho SY, Salerno-Uriarte JA, Tritto M, Spadacini G. Electroanatomic analysis of sinus impulse propagation in normal human atria. *J Cardiovasc Electrophysiol* 2002;**13**:1–10.
2. Schuessler RB, Boineau JP, Bromberg BI. Origin of the sinus impulse. *J Cardiovasc Electrophysiol* 1996;**7**:263–274.
3. Ihara Z, van Oosterom A, Hoekema R. Atrial repolarization as observable during the PQ interval. *J Electrocardiol* 2006;**39**:290–297.
4. Holmqvist F, Carlsson J, Platonov PG. Detailed ECG analysis of atrial repolarization in humans. *Ann Noninvasive Electrocardiol* 2009;**14**:13–18.
5. Holmqvist F, Carlsson J, Waktare JE, Platonov PG. Noninvasive evidence of shortened atrial refractoriness during sinus rhythm in patients with paroxysmal atrial fibrillation. *Pacing Clin Electrophysiol* 2009;**32**:302–307.
6. Gelband H, Bush HL, Rosen MR, Myerburg RJ, Hoffman BF. Electrophysiologic properties of isolated preparations of human atrial myocardium. *Circ Res* 1972;**30**:293–300.
7. Krueger MW, Dorn A, Keller DU, et al. *In-silico* modeling of atrial repolarization in normal and atrial fibrillation remodeled state. *Med Biol Eng Comput* 2013;**51**:1105–1119.
8. Sprague HB, White PD. Clinical observations on the T wave of the auricle appearing in the human electrocardiogram. *J Clin Invest* 1925;**4**:389–402.
9. Ozyigit T, Kocas O, Karadag B, Ozben B. Three dimensional left atrial volume index is correlated with P wave dispersion in elderly patients with sinus rhythm. *Wien Klin Wochenschr* 2016;**128**:182–186.
10. Aniyarajah V, Mercado K, Apiyasawat S, Puri P, Spodick DH. Correlation of left atrial size with p-wave duration in interatrial block. *Chest* 2005;**128**:2615–2618.
11. van Dam PM, Locati ET, Ciconte G, et al. Novel CineECG derived from standard 12-lead ECG enables right ventricle outflow tract localization of electrical substrate in patients with Brugada syndrome. *Circ Arrhythm Electrophysiol* 2020;**13**:e008524.
12. van Dam PM, Boonstra M, Locati ET, Loh P. The relation of 12 lead ECG to the cardiac anatomy: the normal CineECG. *J Electrocardiol* 2021;**69**:67–74.
13. Boonstra MJ, Hilderink BN, Locati ET, Asselbergs FW, Loh P, van Dam PM. Novel CineECG enables anatomical 3D localization and classification of bundle branch blocks. *Europace* 2021;**23**:180–187.
14. van Dam PM, Boonstra M, Roudijk R, et al. ed. The electro-anatomical pathway for normal and abnormal ECGs in COVID patients. 2020 *Computing in Cardiology*, 13–16 September 2020. 2020.
15. van Dam PM. A new anatomical view on the vector cardiogram: the mean temporal-spatial isochrones. *J Electrocardiol* 2017;**50**:732–738.
16. Roberts D, Hersh L, Scher A. Influence of cardiac fiber orientation on wavefront voltage, conduction velocity, and tissue resistivity in the dog. *Circ Res* 1979;**44**:701–712.
17. Kleber AG, Janse MJ, Wilms-Schopmann FJ, Wilde AA, Coronel R. Changes in conduction velocity during acute ischemia in ventricular myocardium of the isolated porcine heart. *Circulation* 1986;**73**:189–198.
18. van Dam PM, Oostendorp TF, van Oosterom A. ECGSIM: interactive simulation of the ECG for teaching and research purposes. *Comput Cardiol* 2010;**37**:841–844.
19. van Dam PM, Oostendorp TF, Linnenbank AC, van Oosterom A. Non-invasive imaging of cardiac activation and recovery. *Ann Biomed Eng* 2009;**37**:1739–1756.
20. Boussejot R, Kreiseler D, Schnabel A. Nutzung der EKG-Signaldatenbank CARDIODAT der PTB über das Internet. *Bionied Technol/Biomed Eng* 2009;**40**:317–318.
21. Badilini F, Libretti G, Yaglio M. Automated JTpeak analysis by BRAVO. *J Electrocardiol* 2017;**50**:752–757.
22. Klugfield P, Badilini F, Denjoy I, et al. Comparison of automated interval measurements by widely used algorithms in digital electrocardiographs. *Am Heart J* 2018;**200**:1–10.
23. Wagner P, Strodthoff N, Boussejot RD, et al. PTB-XL, a large publicly available electrocardiography dataset. *Sci Data* 2020;**7**:154.
24. Rothinger FX, Cheng J, SippensGroenewegen A, et al. Use of electroanatomic mapping to delineate transseptal atrial conduction in humans. *Circulation* 1999;**100**:1791–1797.
25. Markides V, Schilling RJ, Yen Ho S, Chow AWC, Davies DW, Peters NS. Characterization of left atrial activation in the intact human heart. *Circulation* 2003;**107**:733–739.
26. Li Z, Herttervig E, Kongstad O, et al. Global repolarization sequence of the right atrium. *Pacing Clin Electrophysiol* 2003;**26**:1803–1808.
27. Hayashi H, Okajima M, Yamada K. Atrial T (Ta) loop in patients with A-V block: a trial to differentiate normal and abnormal groups. *Ann Heart J* 1976;**91**:492–500.
28. Debbas NMG, Jackson SHD, de Jonghe D, Robert A, Camm AJ. Human atrial repolarization: effects of sinus rate, pacing and drugs on the surface electrocardiogram. *J Am Coll Cardiol* 1999;**33**:358–365.
29. Platonov PG, Mitrofanova L, Ivanov V, Ho SY. Substrates for intra-atrial and interatrial conduction in the atrial septum: anatomical study on 84 human hearts. *Heart Rhythm* 2008;**5**:1189–1195.
30. Holmqvist F, Husser D, Tapanainen JM, et al. Interatrial conduction can be accurately determined using standard 12-lead electrocardiography: validation of P-wave morphology using electroanatomic mapping in man. *Heart Rhythm* 2008;**5**:413–418.